

Supplemental material

Bradley et al., <https://doi.org/10.1084/jem.20181406>

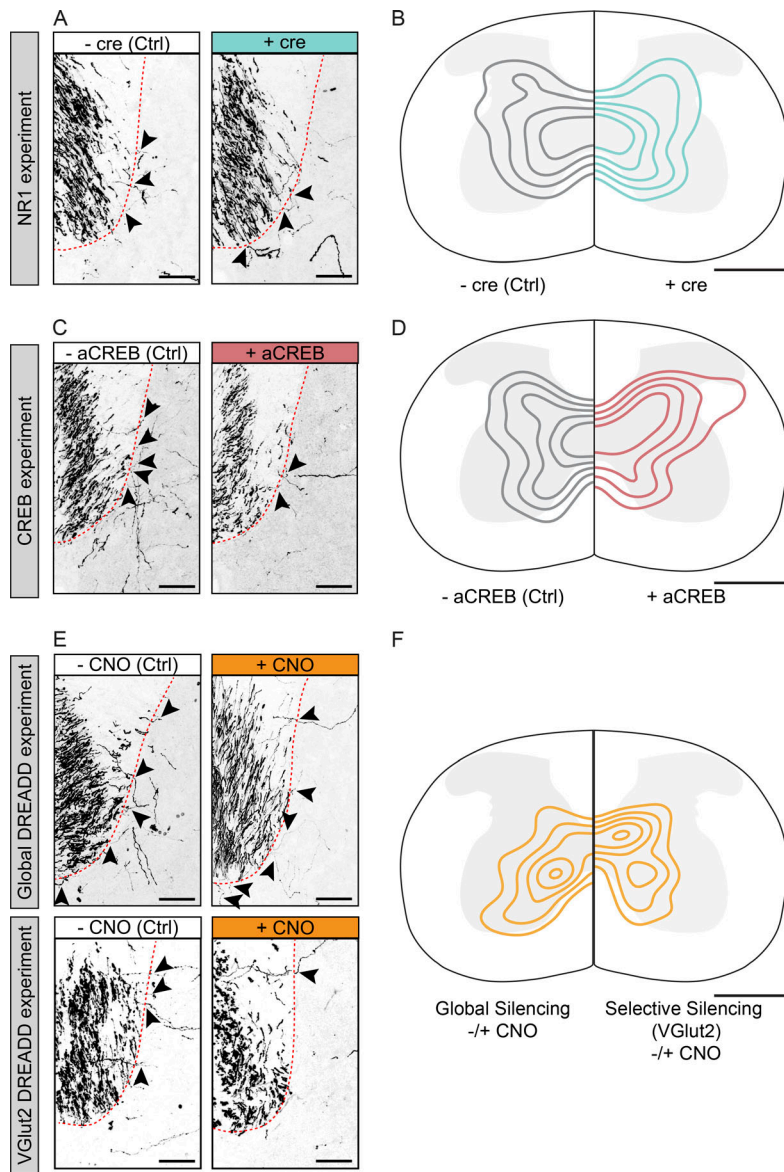


Figure S1. Morphology of CST collaterals and distribution of rAAV-transduced neurons in experiments manipulating activity-dependent signaling.
(A) Confocal images showing exiting CST collaterals (black arrowheads) in the cervical spinal cord (red dashed line indicates white to gray matter border) following genetic ablation of the NR1 subunit of the NMDARs during detour circuit formation (-cre, injected with rAAV-GFP; +cre, injected with rAAV-GFP-Cre; CST, green; GFP⁺ neurons, magenta). **(B)** Representation of the localization of GFP⁺ neurons following injections of rAAV-GFP (-cre) or rAAV-GFP-Cre (+cre) into the spinal cord (level C4) of NR1 floxed mice. **(C)** Confocal images of the cervical spinal cord showing exiting CST collaterals (black arrowheads) following viral delivery of a dominant negative inhibitor of CREB-mediated transcription (aCREB) or control virus (red dashed line indicates white to gray matter border; -aCREB, injected with rAAV-GFP; +aCREB, injected with rAAV-GFP-aCREB). **(D)** Representation of the localization of GFP⁺ neurons following injections of rAAV-GFP (-aCREB) or rAAV-GFP-aCREB (+aCREB) into the spinal cord (level C4) of C57BL6 mice. **(E)** Confocal images of exiting CST collaterals (black arrowheads) following silencing of excitatory and inhibitory neurons in C57BL6 mice (top “Global DREADD experiment”; red dashed line indicates white to gray matter border; -CNO, injected with rAAV-DIO-hM4Di-mCherry and AAV-GFP-Cre and treated with saline; +CNO, injected with rAAV-DIO-hM4Di-mCherry and AAV-GFP-Cre and treated with CNO) and confocal images of exiting CST collaterals (black arrowheads) following silencing of excitatory neurons in VGluT2-cre mice (bottom “VGluT2 DREADD experiment”; red dashed line indicates white to gray matter border; -CNO, injected with rAAV-DIO-hM4Di-mCherry and treated with saline; +CNO, injected with rAAV-DIO-hM4Di-mCherry and treated with CNO). **(F)** Representation of the localization of mCherry⁺ neurons following injections of rAAV-DIO-hM4Di-mCherry and AAV-GFP-Cre (left side; global silencing) into the spinal cord (level C4) of C57BL6 mice or rAAV-DIO-hM4Di-mCherry into the spinal cord (level C4) of VGluT2-cre mice (right side; selective silencing). Ctrl, control. Scale bars, 50 μm in A, C, and E. Scale bars, 5 mm in B, D, and F.

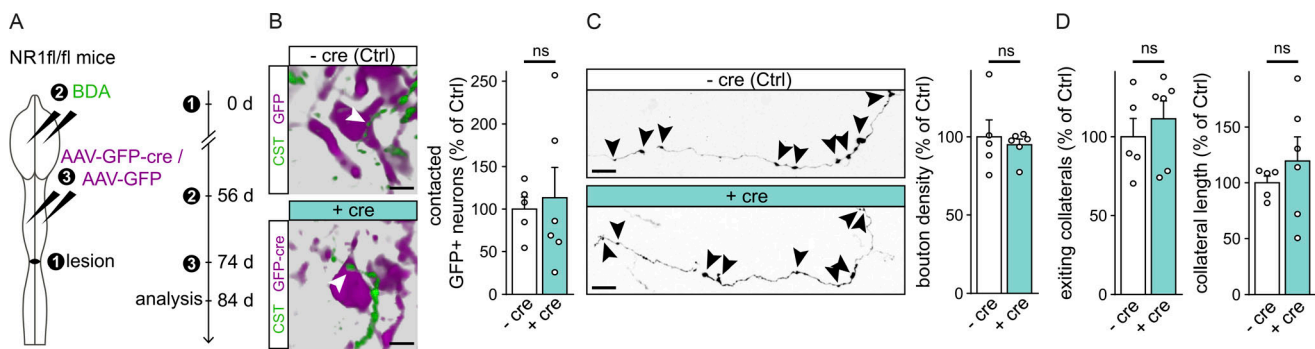


Figure S2. Genetic ablation of the NR1 subunit has no effect on mature rewired circuits. **(A)** Experimental setup of the genetic ablation of the NR1 subunit of the NMDAR in spinal relay neurons of a mature rewired circuit. **(B)** 3D reconstructions of CST contacts on AAV-transfected neurons ($-cre$, injected with rAAV-GFP; $+cre$, injected with rAAV-GFP-Cre; CST, green; GFP $^+$ neurons, magenta; arrowheads indicate contacted cells) and quantification showing that the ablation of the NR1 subunit of the NMDAR in spinal neurons of mature detour circuits has no effect on the proportion of these neurons contacted by CST collaterals ($P = 0.7564$; $n = 5$ or 6 mice per group). **(C)** Confocal images of cervical CST collaterals and quantitative analysis of the bouton density on CST collaterals (arrowheads indicate boutons; $P = 0.6397$; $n = 5$ or 6 mice per group). **(D)** Quantitative analysis of the number (left panel, $P = 0.5023$) and length (right panel, $P = 0.4458$; $n = 5$ or 6 mice per group) of these collaterals in the cervical spinal cord of mice injected with rAAV-GFP ($-cre$) or rAAV-GFP-Cre ($+cre$). Data were analyzed using an unpaired *t* test and presented as mean \pm SEM. Ctrl, control; ns, not significant. Scale bars, 10 μ m in B and C.

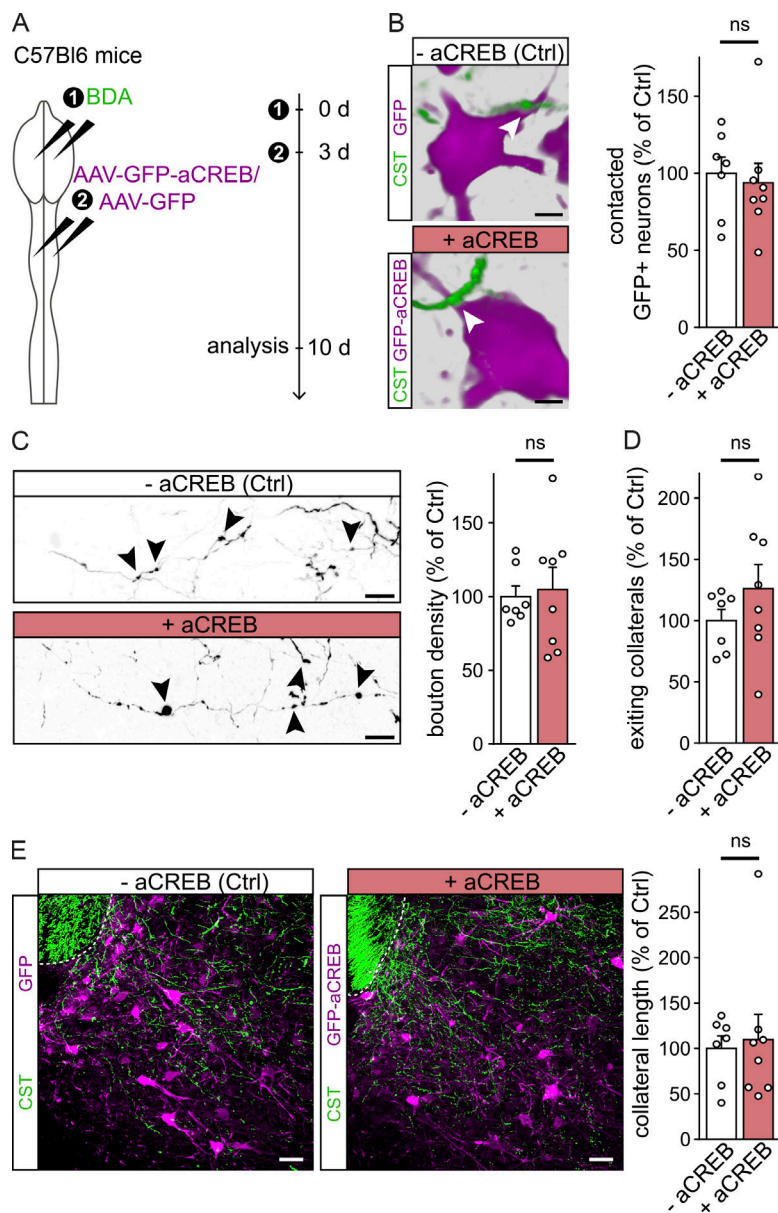


Figure S3. Inhibition of CREB-mediated transcription does not alter uninjured forelimb CST projections. **(A)** Experimental setup of the inhibition of CREB-mediated transcription using viral delivery of a dominant negative inhibitor (aCREB) in uninjured forelimb CST circuits. **(B)** 3D reconstructions of CST contacts on AAV-transfected neurons (-aCREB, injected with rAAV-GFP; +aCREB, injected with rAAV-GFP-aCREB; CST, green; GFP⁺ neurons, magenta; arrowheads indicate contacted cells) and quantification showing that the ablation of CREB-mediated transcription did not change the proportion of these neurons contacted by CST collaterals ($P = 0.7186$, $n = 7$ or 8 mice per group). **(C)** Confocal images of cervical CST collaterals and quantitative analysis of the bouton density on CST collaterals (arrowheads indicate boutons; $P = 0.7830$; $n = 7$ or 8 mice per group). **(D)** Quantitative analysis of the number ($P = 0.2764$; $n = 7$ or 8 mice per group) of these collaterals in the cervical spinal cord of mice injected with rAAV-GFP (-aCREB) or rAAV-GFP-aCREB (+aCREB). **(E)** Confocal images (left panel) of cervical CST collaterals (green) and aCREB-transduced neurons (magenta; arrowheads indicate CST collaterals) and quantitative analysis (right panel) of the length of CST collaterals ($P = 0.7713$, $n = 7$ or 8 mice per group). Data were analyzed using unpaired *t* test and presented as mean \pm SEM. Ctrl, control; ns, not significant. Scale bars, 10 μ m in B and C, and 50 μ m in E.